

1 Supplemental figures and tables for LHCb-PAPER- 2 2023-016

3 The background-subtracted invariant mass distribution of the K^+K^- system is shown in
4 Fig. 1, with the vertical lines indicating the boundaries of six bins. Figure 2 illustrates
5 the Argand plot of the P-wave under the assumption that the S-wave phase is nearly
6 constant in the K^+K^- mass range around the $\phi(1020)$ resonance. Figure 3 indicates the
7 asymmetry between background-subtracted B_s^0 - and \bar{B}_s^0 -tagged decays as a function of
8 the decay time, weighted by the per-candidate mistag probability and the decay-time
resolution effect.

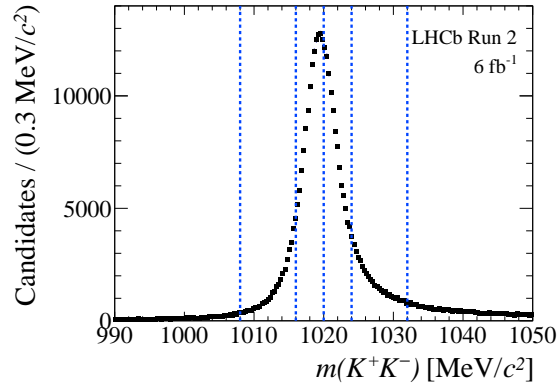


Figure 1: Background-subtracted invariant mass distribution of the K^+K^- system in the selected $B_s^0 \rightarrow J/\psi K^+K^-$ candidates. The vertical lines denote the boundaries of the six bins used in the maximum-likelihood fit.

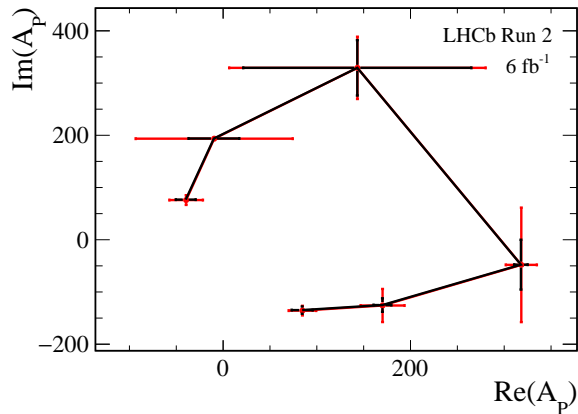


Figure 2: Argand plot of the P-wave, under the assumption that the S-wave phase is constant (or varies very slowly) in the K^+K^- mass range under study. Black error bars represent the statistical uncertainties while red bars represent the total uncertainties.

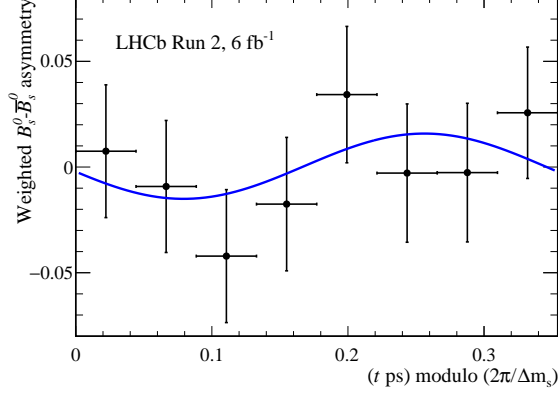


Figure 3: Asymmetry between B_s^0 - and \bar{B}_s^0 -tagged decays as a function of the decay time. The full decay-time range is projected to one oscillation period. The decay candidates are weighted to enhance the visible asymmetry. The blue curve shows the fit projection.

10 The S-wave phases and fractions in the six $m(K^+K^-)$ bins are given by

$$\begin{aligned}
|A_S^1|^2 &= 0.472 \pm 0.024 \pm 0.027, \\
|A_S^2|^2 &= 0.042_{-0.0046}^{+0.0048} \pm 0.010, \\
|A_S^3|^2 &= 0.0029_{-0.0009}^{+0.0013} \pm 0.023, \\
|A_S^4|^2 &= 0.0037_{-0.0019}^{+0.0025} \pm 0.032, \\
|A_S^5|^2 &= 0.0508_{-0.0019}^{+0.0070} \pm 0.027, \\
|A_S^6|^2 &= 0.151 \pm 0.011 \pm 0.051, \\
\delta_S^1 - \delta_\perp &= 2.05_{-0.14}^{+0.12} \pm 0.19 \text{ rad}, \\
\delta_S^2 - \delta_\perp &= 1.62_{-0.19}^{+0.19} \pm 0.41 \text{ rad}, \\
\delta_S^3 - \delta_\perp &= 1.16_{-0.29}^{+0.37} \pm 0.19 \text{ rad}, \\
\delta_S^4 - \delta_\perp &= -0.15_{-0.15}^{+0.12} \pm 0.31 \text{ rad}, \\
\delta_S^5 - \delta_\perp &= -0.637_{-0.076}^{+0.068} \pm 0.17 \text{ rad}, \\
\delta_S^6 - \delta_\perp &= -1.013_{-0.083}^{+0.074} \pm 0.07 \text{ rad},
\end{aligned}$$

11 where the first uncertainty is statistical and the second systematic.

12 The systematic uncertainties for the main physics parameters and the S-wave parameters are summarized in Table 1 and 2, respectively.

14 The correlation matrix used in the combination, can be found in Table 3.

Table 1: Summary of the systematic uncertainties multiplied by 100 for the main physics parameters. The uncertainty of the B_c^+ contamination for $\Delta\Gamma_d^s$ and $\Delta\Gamma_s$ is included in the fit to data and does not contribute to the quoted total systematic uncertainty. DTR refers to decay-time resolution.

Source	$ A_0 ^2$	$ A_\perp ^2$	ϕ_s [rad]	$ \lambda $	$\delta_\perp - \delta_0$ [rad]	$\delta_\parallel - \delta_0$ [rad]	$\Gamma_s - \Gamma_d$ [ps ⁻¹]	$\Delta\Gamma_s$ [ps ⁻¹]	Δm_s [ps ⁻¹]
Mass parametrization	0.04	0.03	0.03	0.02	0.15	0.12	0.02	0.04	0.03
Mass shape statistical	0.04	0.04	0.05	0.09	0.62	0.33	0.02	0.01	0.11
Mass factorization	0.11	0.10	0.42	0.19	0.54	0.60	0.12	0.16	0.18
B_c^+ contamination	0.04	0.05	–	0.02	–	0.17	(0.07)	(0.03)	–
D-wave component	0.04	0.04	0.02	–	0.07	0.13	0.01	0.03	0.02
Ghost tracks	0.07	0.04	0.02	0.10	0.18	0.18	0.02	–	0.01
Multiple candidates	0.01	–	0.27	0.22	0.90	0.41	0.01	0.01	0.24
Particle identification	0.06	0.09	0.27	0.27	1.31	0.51	0.05	0.15	0.46
C_{SP} factors	–	0.01	0.01	0.03	0.73	0.41	–	0.01	0.04
DTR calibration	–	–	0.03	0.02	0.11	0.07	–	–	0.05
DTR model applicability	–	–	0.08	0.03	0.26	0.09	–	–	0.09
Time bias correction	0.04	0.05	0.06	0.05	0.77	0.11	0.03	0.05	0.44
Angular efficiency	0.05	0.14	0.25	0.32	0.42	0.44	0.01	0.02	0.13
Angular resolution	0.01	0.01	0.02	0.01	0.02	0.08	–	0.01	0.02
Kinematic weighting	0.24	0.09	0.01	0.01	0.98	0.86	0.02	0.03	0.31
Momentum uncertainty	0.08	0.04	0.04	–	0.07	0.11	0.01	–	0.13
Longitudinal scale	0.07	0.04	0.04	–	0.10	0.09	0.02	–	0.31
Neglected correlations	–	–	–	–	4.20	4.96	–	–	–
Total systematic uncertainty	0.32	0.24	0.6	0.5	4.8	5.2	0.14	0.24	0.9
Statistical uncertainty	0.17	0.23	2.2	1.1	7.5	6.0	0.14	0.44	3.3

Table 2: Summary of the systematic uncertainties for S-wave parameters. DTR refers to the decay-time resolution.

Source	$\delta_S^1 - \delta_\perp$ [rad]	$\delta_S^2 - \delta_\perp$ [rad]	$\delta_S^3 - \delta_\perp$ [rad]	$\delta_S^4 - \delta_\perp$ [rad]	$\delta_S^5 - \delta_\perp$ [rad]	$\delta_S^6 - \delta_\perp$ [rad]	$ A_S^1 ^2$	$ A_S^2 ^2$	$ A_S^3 ^2$	$ A_S^4 ^2$	$ A_S^5 ^2$	$ A_S^6 ^2$
Mass parametrisation	0.0079	0.0042	0.0139	0.0068	0.0096	0.0101	0.0102	0.0005	0.0001	0.0003	0.0016	0.0038
Mass: shape statistical	0.0082	0.0055	0.0082	0.0036	0.0283	0.0305	0.0108	0.0005	—	0.0001	0.0043	0.0113
Mass factorization	0.0535	0.0092	0.0163	0.0070	0.0072	0.0320	0.0070	0.0007	0.0001	0.0002	0.0007	0.0038
B_c^+ contamination	—	0.24	0.28	0.026	0.20	0.15	—	0.0041	0.00067	—	0.0015	0.0053
D-wave component	0.094	0.17	0.052	0.034	0.017	0.004	0.0043	0.00015	0.00048	—	—	0.00067
Ghost tracks	0.0002	0.0002	0.0001	0.0003	0.0014	0.0009	0.0130	0.0062	0.0016	0.0060	0.0142	0.0013
Multiple candidates	0.026	0.021	0.14	0.0078	0.0053	0.010	0.0090	0.00038	0.00026	0.0011	0.0041	0.0016
Particle identification	0.138	0.026	0.10	0.041	0.033	0.031	0.0106	0.0026	0.0002	0.0002	0.0031	0.0081
C_{sp} factors	0.0743	0.0044	0.0036	0.0012	0.004	0.0437	0.0006	0.0012	0.0002	0.0002	0.0003	0.0023
DTR calibration	0.0008	0.0018	0.0040	0.0007	0.0004	0.0004	—	—	0.0003	—	—	—
DTR model applicability	0.0027	0.0001	0.0019	0.0003	0.0032	0.0020	—	0.0001	—	—	0.0004	0.0004
Time bias correction	0.014	0.0016	0.004	0.005	0.017	0.002	0.0035	0.0007	0.00007	0.0002	0.0002	0.0009
Angular efficiency	0.0072	0.0057	0.0361	0.2368	0.0142	0.0109	0.0027	0.0009	0.0002	0.0005	0.0021	0.0025
Angular resolution	0.0083	0.0015	0.0075	0.0022	0.0021	0.0065	0.0076	—	0.0001	0.0001	0.0002	0.0016
Kinematic weighting	0.0028	0.0012	0.0002	0.0005	0.0024	0.0026	0.0011	0.0061	0.0232	0.0312	0.0212	0.0131
Momentum uncertainty	0.0017	0.0052	0.0009	0.0050	0.0019	0.0014	0.0016	0.0004	—	—	0.0002	0.0010
Longitudinal scale	0.0012	0.0049	0.0019	0.0044	0.0014	0.0015	0.0019	0.0003	—	—	0.0002	0.0009
Neglected correlations	—	—	—	—	0.07	—	—	—	—	—	—	—
Total syst. uncertainty	0.19	0.41	0.19	0.31	0.17	0.07	0.027	0.010	0.023	0.032	0.027	0.051
Statistical uncertainty	0.13	0.19	0.33	0.13	0.072	0.078	0.024	0.0047	0.0010	0.0023	0.0069	0.011

15 The results of the combination of $B_s^0 \rightarrow J/\psi K^+ K^-$ measurements in the $m(K^+ K^-)$
 16 region of the $\phi(1020)$ resonance [1, 2], where the quoted uncertainties include statistical
 17 and systematic sources, yield

$$\begin{aligned}
 \phi_s &= -0.044 \pm 0.020 \text{ rad}, \\
 |\lambda| &= 0.990 \pm 0.010, \\
 \Gamma_s &= 0.6564 \pm 0.0021 \text{ ps}^{-1}, \\
 \Delta\Gamma_s &= 0.0845 \pm 0.0044 \text{ ps}^{-1}, \\
 |A_\perp|^2 &= 0.2471 \pm 0.0032, \\
 |A_0|^2 &= 0.5175 \pm 0.0035, \\
 \delta_\perp - \delta_0 &= 2.924 \pm 0.076 \text{ rad}, \\
 \delta_\parallel - \delta_0 &= 3.150 \pm 0.062 \text{ rad}, \\
 |A_S|^2 &= 0.072 \pm 0.005, \\
 \delta_S - \delta_\perp &= 0.13 \pm 0.25 \text{ rad}, \\
 \Delta m_s &= 17.730 \pm 0.029 \text{ ps}^{-1}, \\
 \tau_d &= 1.515 \pm 0.004 \text{ ps (Gaussian constrained)}, \\
 s &= 0.03 \pm 1.00, \\
 |A_S^1|^2 &= 0.473 \pm 0.036, \\
 |A_S^2|^2 &= 0.042 \pm 0.011, \\
 |A_S^3|^2 &= 0.003 \pm 0.023, \\
 |A_S^4|^2 &= 0.004 \pm 0.032, \\
 |A_S^5|^2 &= 0.051 \pm 0.028, \\
 |A_S^6|^2 &= 0.151 \pm 0.024, \\
 \delta_S^1 - \delta_\perp &= 2.05 \pm 0.23 \text{ rad}, \\
 \delta_S^2 - \delta_\perp &= 1.63 \pm 0.35 \text{ rad}, \\
 \delta_S^3 - \delta_\perp &= 1.16 \pm 0.47 \text{ rad}, \\
 \delta_S^4 - \delta_\perp &= -0.16 \pm 0.28 \text{ rad}, \\
 \delta_S^5 - \delta_\perp &= -0.64 \pm 0.23 \text{ rad}, \\
 \delta_S^6 - \delta_\perp &= -1.02 \pm 0.18 \text{ rad}.
 \end{aligned}$$

18 The parameter s denotes the Gaussian constraint on the fully correlated B_c^+ contribu-
 19 tion between the modes, which is applied on the lifetime parameters. The p-value of the
 20 fit is 0.2. The full correlation matrix is given in Table 4.

21 The results of the combination of all LHCb ϕ_s measurements [1–7], where the quoted

22 uncertainties include statistical and systematic sources, are

$$\begin{aligned}
\phi_s &= -0.031 \pm 0.018 \text{ rad}, \\
|\lambda| &= 0.990 \pm 0.010, \\
\Gamma_s &= 0.6563 \pm 0.0020 \text{ ps}^{-1}, \\
\Delta\Gamma_s &= 0.0846 \pm 0.0039 \text{ ps}^{-1}, \\
|A_\perp|^2 &= 0.2471 \pm 0.0031, \\
|A_0|^2 &= 0.5175 \pm 0.0035, \\
\delta_\perp - \delta_0 &= 2.94 \pm 0.07 \text{ rad}, \\
\delta_\parallel - \delta_0 &= 3.150 \pm 0.062 \text{ rad}, \\
|A^S|^2 &= 0.072 \pm 0.045, \\
\delta_S - \delta_\perp &= 0.13 \pm 0.25 \text{ rad}, \\
\Delta m_s &= 17.740 \pm 0.027 \text{ ps}^{-1}, \\
\tau_d &= 1.5152 \pm 0.0035 \text{ ps (Gaussian constrained)}, \\
s &= 0.03 \pm 1.00, \\
|A_S^1|^2 &= 0.473 \pm 0.036, \\
|A_S^2|^2 &= 0.042 \pm 0.011, \\
|A_S^3|^2 &= 0.003 \pm 0.023, \\
|A_S^4|^2 &= 0.004 \pm 0.032, \\
|A_S^5|^2 &= 0.051 \pm 0.028, \\
|A_S^6|^2 &= 0.151 \pm 0.024, \\
\delta_S^1 - \delta_\perp &= 2.05 \pm 0.23 \text{ rad}, \\
\delta_S^2 - \delta_\perp &= 1.62 \pm 0.35 \text{ rad}, \\
\delta_S^3 - \delta_\perp &= 1.16 \pm 0.47 \text{ rad}, \\
\delta_S^4 - \delta_\perp &= -0.16 \pm 0.28 \text{ rad}, \\
\delta_S^5 - \delta_\perp &= -0.64 \pm 0.23 \text{ rad}, \\
\delta_S^6 - \delta_\perp &= -1.02 \pm 0.18 \text{ rad}, \\
|\lambda^{J/\psi\pi\pi}| &= 0.926 \pm 0.046, \\
|\lambda^{\text{HM}}| &= 0.994 \pm 0.019, \\
|\lambda^{\psi(2S)}| &= 1.046 \pm 0.069, \\
|A_\perp^{\psi(2S)}|^2 &= 0.253 \pm 0.018, \\
|A_0^{\psi(2S)}|^2 &= 0.426 \pm 0.011, \\
\delta_\parallel^{\psi(2S)} - \delta_0^{\psi(2S)} &= 3.69 \pm 0.18 \text{ rad}, \\
\delta_\perp^{\psi(2S)} - \delta_0^{\psi(2S)} &= 3.32 \pm 0.43 \text{ rad}, \\
|A_S^{\psi(2S)}|^2 &= 0.056 \pm 0.026, \\
\delta_S^{\psi(2S)} &= 0.02 \pm 0.14 \text{ rad}, \\
|\lambda^{D_s^+ D_s^-}| &= 0.91 \pm 0.18,
\end{aligned}$$

23 where the indices $J/\psi\pi\pi$, HM (high-mass), $\psi(2S)$ and $D_s^+D_s^-$ denote parameters obtained
 24 from the measurements of $B_s^0 \rightarrow J/\psi\pi^+\pi^-$, $B_s^0 \rightarrow J/\psi K^+K^-$ in the region above the
 25 $\phi(1020)$ resonance, $B_s^0 \rightarrow \psi(2S)K^+K^-$ and $B_s^0 \rightarrow D_s^+D_s^-$, respectively. The p -value of
 26 the fit is 0.3. The full correlation matrix is given in Table 5. The individual results and
 27 their average are shown in Fig. 4.

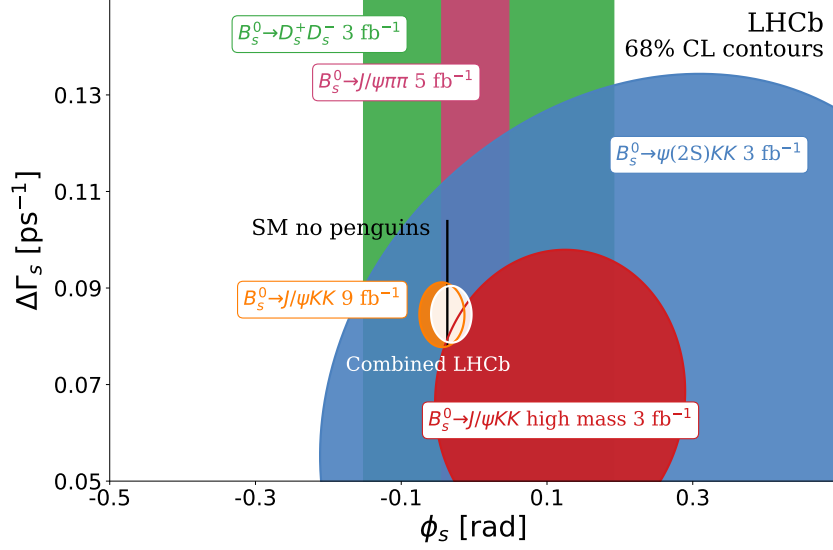


Figure 4: Summary of LHCb measurements of ϕ_s and, wherever applicable, $\Delta\Gamma_s$, in $b \rightarrow c\bar{c}s$ transitions and their average.

28 The results presented in the Letter, in the form of a json file and as used in the
 29 combination, are added as Supplemental Material [8]. The file includes all central values,
 30 statistical and systematic uncertainties and correlations.

References

- [1] LHCb collaboration, R. Aaij *et al.*, *Precision measurement of CP violation in $B_s^0 \rightarrow J/\psi K^+ K^-$ decays*, Phys. Rev. Lett. **114** (2015) 041801, arXiv:1411.3104.
- [2] LHCb collaboration, R. Aaij *et al.*, *First measurement of the CP-violating phase in $B_s^0 \rightarrow J/\psi(e^+e^-)\phi$ decays*, arXiv:2105.14738, to appear in EPJC.
- [3] LHCb collaboration, R. Aaij *et al.*, *Resonances and CP-violation in B_s^0 and $\bar{B}_s^0 \rightarrow J/\psi K^+ K^-$ decays in the mass region above the $\phi(1020)$* , JHEP **08** (2017) 037, arXiv:1704.08217.
- [4] LHCb collaboration, R. Aaij *et al.*, *Measurement of the CP-violating phase ϕ_s in $\bar{B}_s^0 \rightarrow D_s^+ D_s^-$ decays*, Phys. Rev. Lett. **113** (2014) 211801, arXiv:1409.4619.
- [5] LHCb collaboration, R. Aaij *et al.*, *Measurement of the CP-violating phase ϕ_s in $\bar{B}_s^0 \rightarrow J/\psi \pi^+ \pi^-$ decays*, Phys. Lett. **B736** (2014) 186, arXiv:1405.4140.
- [6] LHCb collaboration, R. Aaij *et al.*, *Measurement of the CP violating phase and decay-width difference in $B_s^0 \rightarrow \psi(2S)\phi$ decays*, Phys. Lett. **B762** (2016) 253, arXiv:1608.04855.
- [7] LHCb collaboration, R. Aaij *et al.*, *Updated measurement of time-dependent CP-violating observables in $B_s^0 \rightarrow J/\psi K^+ K^-$ decays*, Eur. Phys. J. **C79** (2019) 706, Erratum *ibid.* **C80** (2020) 601, arXiv:1906.08356.
- [8] *See Supplemental Material at [link inserted by publisher] for a summary of systematic uncertainties and numerical results and additional plots for the fit result and combinations of LHCb measurement.*